

THE STRUCTURE OF ^{26}Mg INVESTIGATED WITH THE (d, p) REACTION

H. F. R. ARCISZEWSKI, E. A. BAKKUM, C. P. M. VAN ENGELEN, P. M. ENDT
and R. KAMERMANS

Fysisch Laboratorium, Rijksuniversiteit Utrecht, PO Box 80.000, 3508 TA Utrecht, The Netherlands

Received 14 May 1984

(Revised 4 July 1984)

Abstract: Angular distributions have been measured for the $^{25}\text{Mg}(\text{d}, \text{p})^{26}\text{Mg}$ reaction at 13 MeV leading to excited states between $E_x = 0$ and 8 MeV. Experimental cross sections are compared with DWBA calculations and extended shell-model calculations in the full sd shell. Spin and parity restrictions are obtained for several levels in the region $E_x = 6\text{--}8$ MeV. Spectroscopic factors for transitions to the lowest four positive-parity states of each spin are well reproduced by the shell-model calculations; however, in mixed configurations the largest component is systematically underestimated by the shell model. Only 60% of the strength for $s_{1/2}$ transfer is observed.

E

NUCLEAR REACTIONS $^{25}\text{Mg}(\text{d}, \text{p})$, $E = 13$ MeV; measured $\sigma(E(\text{p}), \theta)$. Magnetic spectrograph, gas-ionization chamber. DWBA analysis, shell-model calculations.

1. Introduction

At the moment a very complete comparison between shell-model calculations and experimental data can be made in the mass region around $A = 26$. Especially for ^{26}Al the amount of experimental data is extensive and precise. At higher energies (above 6 MeV excitation energy, approximately), however, some experimental information is still lacking. While (p, γ) experiments involving ^{26}Al are currently being undertaken¹), a detailed investigation of its isobaric neighbour ^{26}Mg , on which experimental information is less abundant, would yield valuable information about the $T = 1$ states in ^{26}Al . The $^{25}\text{Mg}(\text{d}, \text{p})^{26}\text{Mg}$ single-particle transfer reaction at $E_d = 13$ MeV was chosen, since this type of reaction can be well described by standard direct-reaction theory and exhibits angular distributions which are very sensitive with respect to the angular momentum transferred. In this way, spectroscopic factors and information on the J^π of the excited states in ^{26}Mg can be obtained. A disadvantage is the fact that the ground state of the target nucleus ^{25}Mg has $J^\pi = \frac{5}{2}^+$, which is added vector-wise to the transferred angular momentum. For this reason the information on the spin of the excited states from this reaction will be rather restricted.

Extended shell-model calculations in the full sd shell were performed in order to investigate the accuracy of the wave functions. The wave functions were calculated by the programme RITSSCHIL²⁾ using the Chung-Wildenthal interaction³⁾. It appeared that the first four positive-parity states of each spin were reproduced rather well, both for the excitation energy and the spectroscopic factors for the neutron-stripping reaction on ^{25}Mg .

2. Experimental procedure

The $^{25}\text{Mg}(d, p)^{26}\text{Mg}$ reaction has been studied at an incident energy of 13 MeV. The deuterons were accelerated by the 7 MV EN tandem Van de Graaff accelerator of the Utrecht university with beam currents in the order of 100 nA. Angular distributions of the reaction protons were measured with two types of targets: at angles larger than 15° a target of $108 \mu\text{g}/\text{cm}^2$ ^{25}Mg evaporated on a $615 \mu\text{g}/\text{cm}^2$ Au foil was used, whereas for smaller angles the target consisted of $110 \mu\text{g}/\text{cm}^2$ ^{25}Mg on a $20 \mu\text{g}/\text{cm}^2$ carbon backing. This last backing was chosen in order to prevent a too-high count rate due to deuterons elastically scattered from Au. Both targets were enriched in ^{25}Mg to more than 99%.

The reaction protons were detected in a gas-filled detector of the type developed in Rochester⁴⁾, which was positioned in the focal plane of an Enge split-pole magnetic spectrograph. The detector was positioned at an angle of 42° with respect to the focal plane so that the average ejectile trajectory is perpendicular to the two proportional counters in the detector. Because the protons are only lightly ionising, isobutane with its relatively large stopping power was used as detector gas in order to obtain a maximal primary ionization. Nevertheless, the signals from the ΔE and E anodes in the detector could not be used for particle identification. The difference in energy loss of the protons and the deuterons below the proportional counters was large enough, however, to achieve a clear particle identification. The proportional counters consist of a NiCr resistive anode wire to enable a charge-division position readout. From the position readout of the two proportional counters, which are placed at a distance of 10 cm from each other, the particle position along the focal plane of the spectrograph can be determined. In order to improve the position resolution, the cathode of the first proportional counter was replaced by a striped cathode directly coupled to a discrete delay line⁵⁾. The installation of the delay-line readout system improved the position resolution along the focal plane from 1.5 mm to less than 1 mm, yielding an energy resolution of about 25 keV. Towards both edges of the detector the energy resolution degraded to about 35–40 keV, an effect which is mainly due to the extrapolation procedure required to extract the focal-plane position from the position readouts of the proportional counters, and to the worse position resolution of the second counter. Replacement of this second counter by a delay-

line readout system is of little use, since its position resolution at 11 cm distance from the entrance foil is mainly determined by angular straggling in the foil and in the detector gas-filling. Since for lightly ionising particles the position (energy) resolution is directly determined by the signal-to-noise ratio of the proportional-counter pulses, the counters had to be operated at a high gas pressure (270 Torr) as well as with a high multiplication factor. This last condition implied that the voltages applied should be as high as possible, in practice around 1500 V. A drawback of operating the detector under such conditions was the fact that cracking products of the isobutane tended to pollute and subsequently disable the anode wires rather fast. For this reason the detector count rate was kept low, at about 100 counts/sec, in order to minimize the pollution rate.

The position as well as the energy signals from both proportional counters were digitized and transported via a CAMAC system to a PDP 11/34 on-line computer, which subsequently wrote them to tape for off-line analysis. From the data the following quantities were extracted: the positions s_1 and s_2 along the two proportional counters, the energy losses ΔE_1 and ΔE_2 of the particles below the proportional counters, the position ρ along the (software defined) focal plane, and the angle of incidence θ in the detector. During the experiment the momentum spectra of the protons (ρ) and two-dimensional $\Delta E_i \times s_i$ (energy-loss versus position) "twinkle frames" were used for monitoring purposes. In the off-line analysis proton (ρ) spectra were constructed from those events which fulfilled the following (software) conditions: (a) they belonged to the proton groups as defined by a two-dimensional window in the $\Delta E_1 \times s_1$ matrix, and (b) they followed the correct trajectory in the spectrograph as defined by a two-dimensional window in the $\rho \times \theta$ matrix.

The angular distributions were measured in steps of 5° between $\theta_{\text{lab}} = 5^\circ$ and $\theta_{\text{lab}} = 50^\circ$. At larger angles contributions from compound nucleus formation are expected to become important. The distance along the focal plane covered by the detector in this particular setup corresponds to about 5 MeV in excitation energy. Therefore at each angle two measurements were made with two different field settings of the spectrograph, covering an energy region up to around 8 MeV in excitation energy. This procedure moreover ensured that the main region of interest, around 5 to 6 MeV in excitation energy, was measured twice, with good position resolution in both cases. The relative normalization of the different runs was obtained in two ways: first by monitoring deuterons elastically scattered from ^{25}Mg with a Si detector positioned at a fixed angle of 45° , and secondly by means of a Faraday cup connected to a current integrator measuring the total collected charge. Both methods were found to be in agreement within 2%. The dead time of the data-acquisition system and the electronics was determined using a pulser signal, externally triggered by the current integrator, connected to the test inputs of the detector preamplifiers. A comparison between the total number of trigger pulses and the amount of pulser signals registered on magnetic tape, gives the total dead time, which was found to be less than 1% for all angles.

Absolute cross sections for the $^{25}\text{Mg}(\text{d}, \text{p})^{26}\text{Mg}$ reaction were obtained from deuteron elastic-scattering data measured with the same experimental setup. The target thickness and the solid angle of the spectrograph were calibrated by comparing the measured cross section of the $^{25}\text{Mg}(\text{d}, \text{d}_0)^{25}\text{Mg}$ reaction at $\theta_{\text{lab}} = 15^\circ$ and $\theta_{\text{lab}} = 20^\circ$ with optical-model calculations for this reaction. The elastic-scattering cross sections at these angles can be calculated with an accuracy of about 10%, from which it follows that the absolute $^{25}\text{Mg}(\text{d}, \text{p})^{26}\text{Mg}$ cross sections are accurate to about the same degree.

3. Data analysis

Two proton spectra of the $^{25}\text{Mg}(\text{d}, \text{p})^{26}\text{Mg}$ reaction, measured at an angle $\theta_{\text{lab}} = 25^\circ$, are shown in fig. 1, one for the region of low-excitation energy and one for the higher-energy region. Final states up to an excitation energy of 8 MeV could be observed. All peaks were identified either as belonging to ^{26}Mg or as to the contaminants ^{12}C and ^{16}O . Even states in ^{25}Mg were observed in spite of the low abundance of ^{24}Mg (less than 1%). Most of the ^{26}Mg peaks could be resolved with the exception of the 4.3 MeV, 7.3 MeV, 7.4 MeV and 7.6 MeV doublets or triplets. From these multiplets only the 7.4 MeV triplet, which consists of the 7.350, 7.369 and 7.396 MeV states, could be successfully analysed keeping the known peak positions fixed. This detailed analysis was only possible because of the fact that the transfers to the 7.369 and the 7.396 MeV state appeared to be very weak and therefore only had a marginal effect on the intensity of the transfer to the 7.350 MeV state. In all other multiplets the intensities were found to be of the same order of magnitude and could therefore not be extracted separately. For all peaks a gaussian shape on a constant or linear background was assumed. A comparison with manual integrations of some peaks showed that deviations stay within the errors, although the fitting procedure tended to underestimate the peak area slightly for the smaller peaks.

4. DWBA analysis

The theoretical transfer cross sections were calculated within zero-range DWBA, with the computer programme DWUCK4⁶⁾. Although the dependence of the magnitude of the cross sections and the shape of the diffraction patterns on the optical-model parameters is small, some effort has been put in finding an optimal set. As a starting point two frequently used sets were taken, as determined by Perey and Perey⁷⁾ and Becchetti and Greenlees⁸⁾ for the deuteron entrance channel and the proton exit channel, respectively. No better set could be found, however. The parameter sets used are summarized in table 1. The bound-state

TABLE
Optical-model

Particle	V_0 [MeV]	r_0 [fm]	a_0 [fm]	W_D [MeV]	r_w [fm]	a_w [fm]
protons ^{a)}	$56.6-0.32E_p$	1.17	0.75	$12.3-0.25E_p$	1.32	0.54
deuterons ^{b)}	93.8	1.00	0.87	29.2	1.36	0.61

^{a)} Becchetti-Greenlees ⁶⁾. ^{b)} Perey-Perey ⁷⁾.

wave function of the transferred neutron was generated with a spherical Woods-Saxon potential with a radius parameter $r_0 = 1.25$ fm and diffuseness $a_0 = 0.65$ fm. The depth of the potential well is adjusted in order to obtain the proper binding energy. As usual a Thomas-type potential with $\lambda = 25$

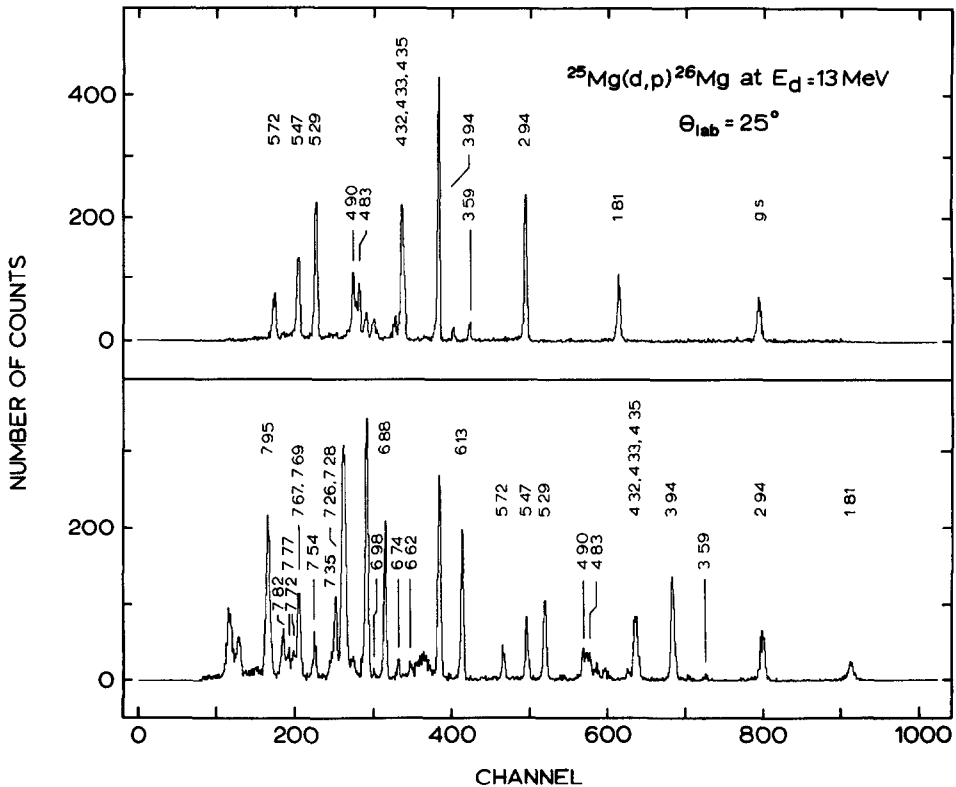


Fig. 1. Proton spectra from the $^{25}\text{Mg}(d,p)^{26}\text{Mg}$ reaction at $\theta_{\text{lab}} = 25^\circ$, measured at two different field settings of the magnetic spectrograph. The ^{25}Mg peaks are labelled with the excitation energies. All other peaks are contaminants.

1

parameters

$V_{s.o.}$ [MeV]	$r_{s.o.}$ [fm]	$a_{s.o.}$ [fm]	r_{Coul} [fm]
6.2	1.01	0.75	1.37
12.0	1.00	0.87	1.30

($r_{s.o.} = 1.25$ fm, $a_{s.o.} = 0.65$ fm) was taken for the spin-orbit interaction. No non-locality or finite-range corrections were included in the final results since no improvement in the description of the shape of the angular distributions was observed. Only the magnitude of the absolute cross sections for $l = 0$ and $l = 2$ transfers increases by about 20% if the corrections are applied. At this incident energy all angular distributions show a clear diffraction pattern as can be seen in figs. 2 to 4. Because the difference, especially at forward angles, between the angular distributions for the different l -transfers is large, unambiguous l -assignments were possible in all cases. A good description of the angular distributions can be obtained as is clear from those cases where only a single l -transfer plays a role, e.g. the $l = 0$ transfer to the 2.938 MeV 2^+ level (which is expected to be a relatively pure $s_{\frac{1}{2}}$ state), and the $l = 2$ transfers to the 0^+ ground state and the 4^+ level at 5.474 MeV, which can only be transfers to a $d_{\frac{3}{2}}$ or $d_{\frac{5}{2}}$ state. Because of this good description and the fact that the maxima of $l = l_1$ and $l = l_1 + 2$ transfers are clearly separated, mixed transfers can be treated with a good amount of confidence. A good example to support this is the transfer to the 6.878 MeV 3^- level which is excellently described by a combination of $l = 1$ and $l = 3$ transfers. However, since the $l = 0$ (or $l = 1$) component is mainly fixed by the part of the angular distribution curve at small angles, which is an order of a magnitude larger than the intermediate-angle part, a small shift of this curve is reflected in a large shift in the remaining $l = 2$ (or $l = 3$) component. This uncertainty in the absolute magnitude of the $l = 2$ or $l = 3$ component is reflected in the large errors of more than 30% as compared to the 10% normally assigned, as derived from the uncertainty in the fit. The experimental error usually is negligible compared to this procedural one.

The relation between calculation and experiment is given by

$$\left(\frac{d\sigma}{d\Omega}\right)_{\text{exp}} = 1.55 S \frac{2J_f + 1}{2J_i + 1} \frac{\sigma_{\text{DWUCK}}}{2j_{\text{transf}} + 1},$$

where J_i and J_f are the total angular momentum of the initial and final state, respectively, and j_{transf} represents the total angular momentum transferred by the neutron. Values for the spectroscopic factor S are summarized in table 2. Because

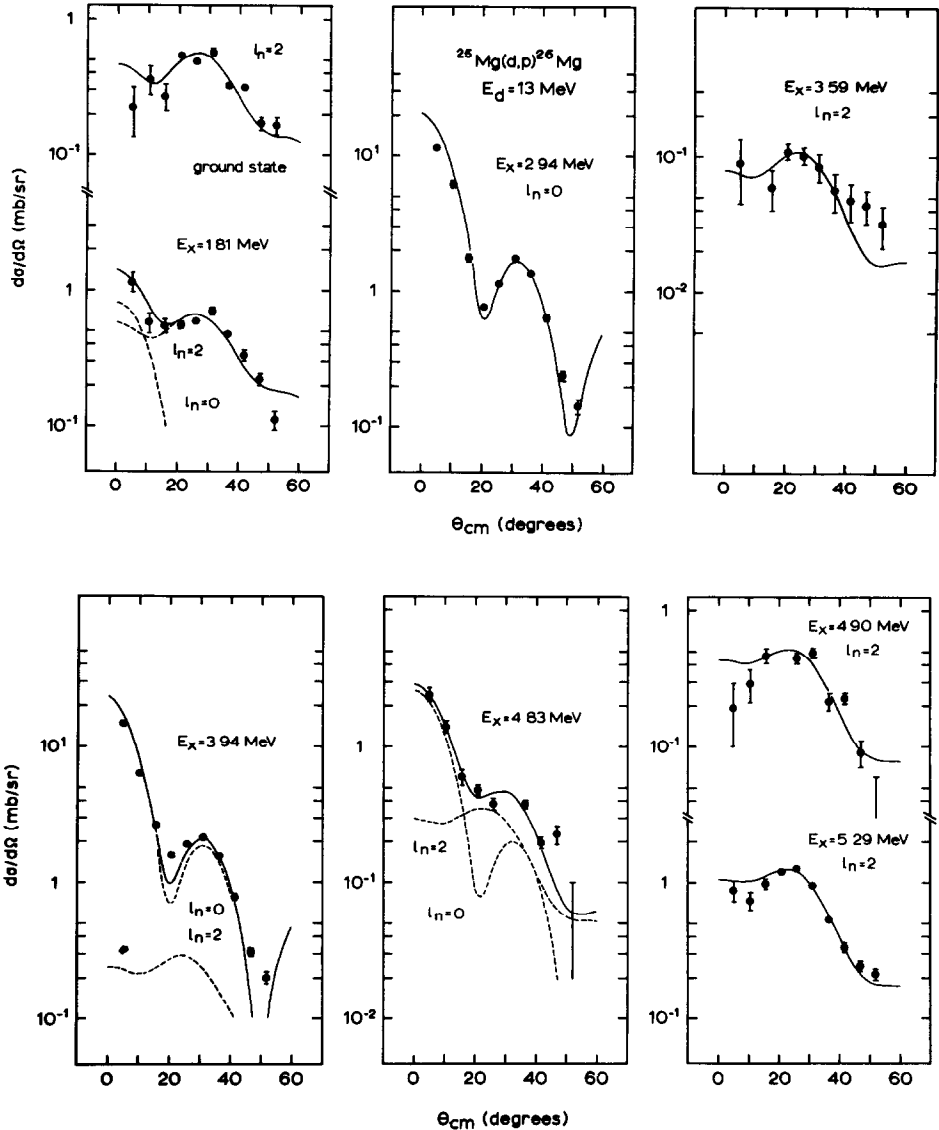


Fig. 2. Proton angular distributions from the $^{25}\text{Mg}(d,p)^{26}\text{Mg}$ reaction at $E_d = 13$ MeV. The full lines represent the total cross sections, while dashed lines (if present) indicate the different l -transfers contributing to the total cross section.

the neutron transfers are mainly dependent on l , experimentally no distinction can be made between transfers which only differ in spin orientation. Therefore only the spectroscopic factor for the most probable final single-neutron state is given (i.e. the $1p_{3/2}$ and $0f_{7/2}$ states for $l = 1$ and $l = 3$ transfers, respectively). The other cross

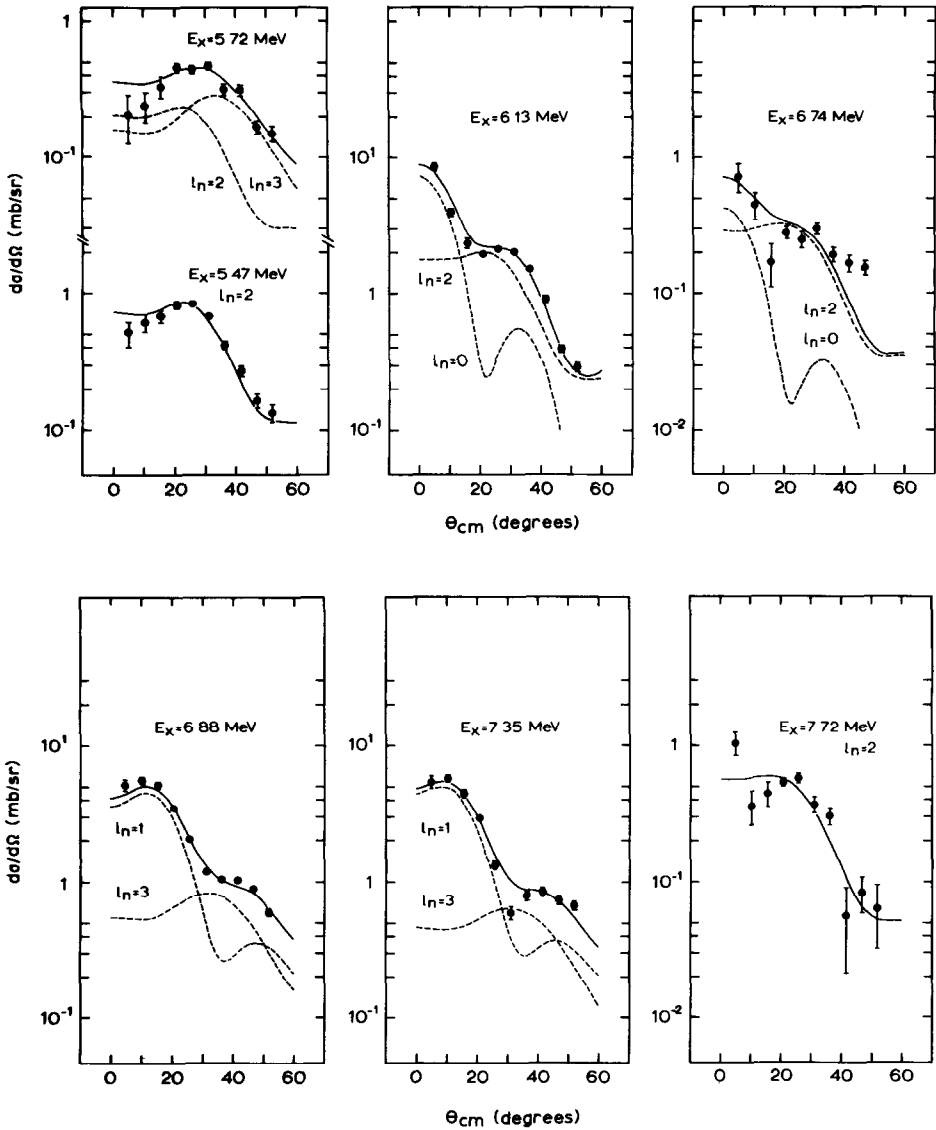


Fig. 3. Same as fig. 2. Note that the $l = 3$ part indicated for the 5.72 MeV cross section necessarily is a transfer to another level close by. See text.

sections only differ by a constant factor from those given. For $l = 2$ transfers, for example, one has

$$\left(\frac{d\sigma}{d\Omega}\right)_{d_{5/2}} = 1.19 \left(\frac{d\sigma}{d\Omega}\right)_{d_{3/2}} .$$

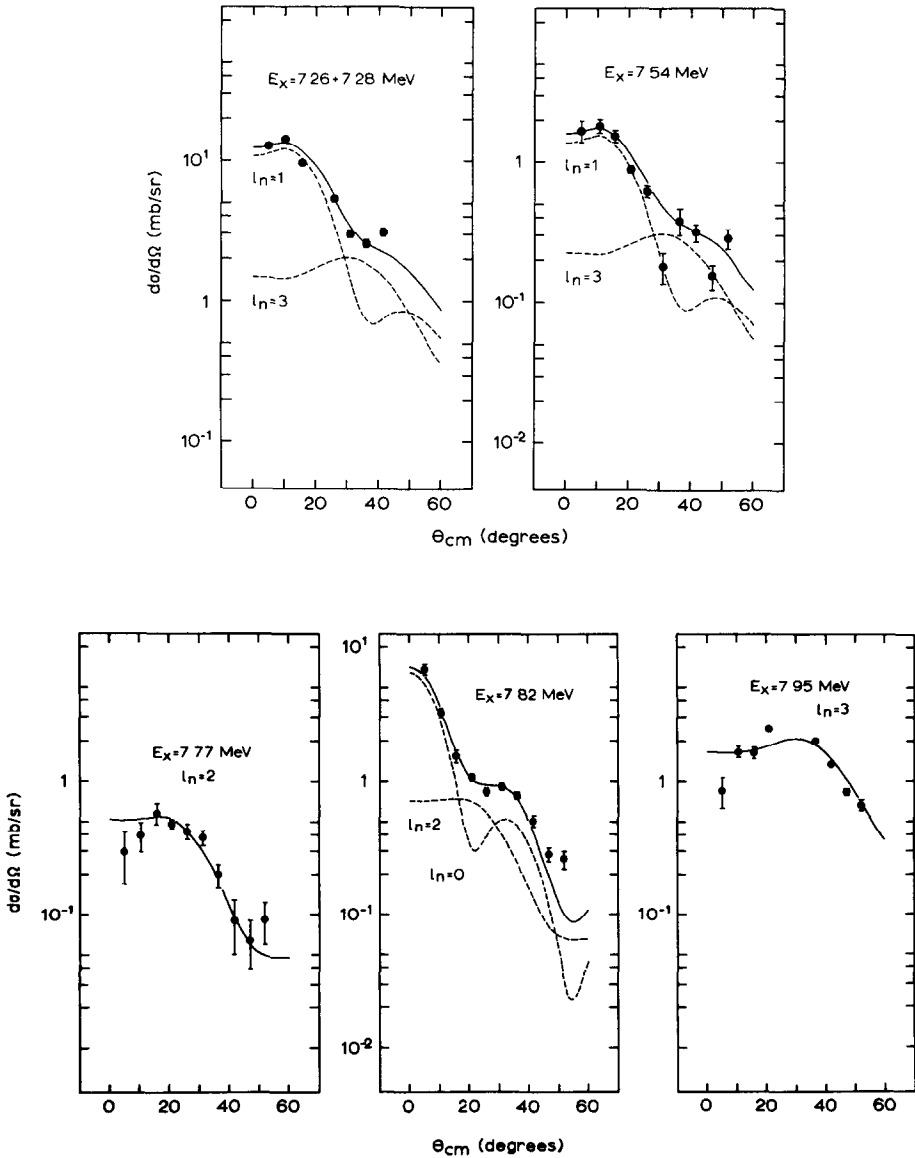


Fig. 4. Same as fig. 2.

Where J^π values were known from previous work⁹⁾ the deduced l -values are in agreement. Only the transfer to the 5.716 MeV 4^+ level is not described well by a pure $l = 2$ transfer. A contribution of an $l = 3$ term produces a much better fit, but this would imply that another ^{26}Mg state must be involved. The only candidate known, the 5.690 MeV level, should have $J = 1$, or possibly $J^\pi = 2^+$ [ref. 9)].

TABLE 2
Spectroscopic factors deduced from the DWBA analysis

E_x [MeV] ^{a)}	J^π ^{b)}	l_n	Assumed single-neutron state	$(2J+1)S$
0	0^+	2	$d_{5/2}$	2.81 ± 0.30
1.809	2^+	0	$s_{1/2}$	0.16 ± 0.05
		2	$d_{3/2}$	3.51 ± 0.35
2.938	2^+	0	$s_{1/2}$	3.37 ± 0.30
3.588	0^+	2	$d_{5/2}$	0.32 ± 0.03
3.941	3^+	0	$s_{1/2}$	1.98 ± 0.20
		2	$d_{3/2}$	1.1 ± 0.5
4.834	2^+	0	$s_{1,2}$	0.30 ± 0.05
		2	$d_{3/2}$	1.05 ± 0.35
4.900	4^+	2	$d_{3/2}$	1.48 ± 0.15
5.291	2^+	2	$d_{3/2}$	3.29 ± 0.30
5.474	4^+	2	$d_{3/2}$	2.15 ± 0.25
5.716	4^+	2	$d_{3/2}$	0.56 ± 0.20
6.125	3^+ ^{d)}	0	$s_{1/2}$	0.74 ± 0.09
		2	$d_{3/2}$	4.2 ± 1.0
6.744	2^+	0	$s_{1/2}$	0.04 ± 0.02
		2	$d_{3/2}$	0.58 ± 0.20
6.878	3^-	1	$p_{3/2}$	1.18 ± 0.15
	3^-		$f_{7/2}$	3.5 ± 1.0
7.262 + 7.282	$(2, 3)^-$ ^{e)}	1	$p_{3/2}$	1.48 ± 0.20
		3	$f_{7/2}$	3.7 ± 1.5
7.347 ^{c)}	3^- ^{e,*)}	1	$p_{3/2}$	1.14 ± 0.15
		3	$f_{7/2}$	2.4 ± 0.8
7.543	$(2, 3)^-$ ^{f,*)}	1	$p_{3/2}$	0.36 ± 0.06
		3	$f_{7/2}$	1.1 ± 0.4
7.723	$(0-5)^+$ ^{f)}	2	$d_{3/2}$	0.80 ± 0.15
7.771	$(0-5)^+$ ^{f)}	2	$d_{3/2}$	0.72 ± 0.07
7.815	$(2, 3)^+$ ^{f)}	0	$s_{1/2}$	0.62 ± 0.06
		2	$d_{3/2}$	0.93 ± 0.15
7.950	$(5, 6)^-$ ^{f)}	3	$f_{7/2}$	7.8 ± 0.8

a) Ref. ⁹⁾.

b) Ref. ⁹⁾, unless indicated otherwise.

c) Ref. ¹²⁾.

d) Ref. ⁹⁾, unnatural parity from ref. ¹⁰⁾.

e) Present work, natural parity from ref. ¹¹⁾.

f) Present work.

*) Further restrictions from (n, γ) work, see ref. ¹³⁾.

This last possibility is in contradiction with the odd parity implied by the $l = 3$ transfer, however. Therefore we tentatively take $J^\pi = 1^-$ for the 5.690 MeV level. Although the transitions to the 7.262 MeV and 7.282 MeV levels could not be separated, their sum has a clear $l = 1$ component, which can be ascribed mainly to the transition to the 7.262 MeV level. Therefore we tentatively assign $J^\pi = (1-4)^-$ to this level. Because of the large uncertainty in the other component(s) of the angular distribution curve, no such assignment is possible for the 7.282 MeV level.

The transfers to the 7.347 MeV and 7.543 MeV levels both have an $l = 1$ and an $l = 3$ component present, confining the spins of these levels to $(1-4)^-$. A recent (t, p) experiment on ^{24}Mg [ref. ¹⁰], in which the transition to the 7.347 MeV level is strongly present, indicates that this level has natural parity, restricting its spin to $J^\pi = (1, 3)^-$. The transitions to the 7.723 MeV, 7.771 MeV and 7.815 MeV levels all unambiguously have $l = 2$, therefore they must have positive parity. The mixing of an $l = 0$ component in the transition to the 7.815 MeV level confines the spin of this level to $(2, 3)^+$, while the absence of such a component makes these spins less probable for the other two levels. The transfer to the 7.950 MeV level to conclude with, has $l = 3$, implying odd parity for this last level. The absence of an $l = 1$ term would seem to point to $J^\pi = (5, 6)^-$, a negative-parity $J = 0$ level implying a too large spectroscopic factor for the transfer, as will be shown later (see table 2).

5. Comparison with shell-model calculations

Shell-model calculations using the Chung-Wildenthal interaction ³⁾ have been performed in the full sd shell. The programme RITSSCHIL ²⁾ was used to calculate the eigenstates of the hamiltonian. In the calculations the ^{16}O core was kept inert, while the ten remaining nucleons were left with no restrictions in the $s_{\frac{1}{2}}$, $d_{\frac{3}{2}}$ and $d_{\frac{5}{2}}$ shells. In this model space only positive-parity states can be considered, since negative-parity states necessarily involve either the $0f_{\frac{7}{2}}$ or the $1p_{\frac{3}{2}}$ orbit, or hole creation in the ^{16}O core. Even so, the diagonalisation of the matrix (with dimensions up to around 5000) already took several hours to complete on a CDC Cyber 175 for the lowest four states for each of the possible spins. Therefore inclusion of $f_{\frac{7}{2}}$ or $p_{\frac{3}{2}}$ excitations is not possible without arbitrary restrictions on the configurations in the sd shell.

A comparison between the calculated level scheme and experiment is presented in fig. 5. The calculated levels extend to about 7 MeV in excitation energy. Because of the large number of known 2^+ levels, the calculations were extended to include the first six levels with $J^\pi = 2^+$. As can be seen from the figure, the experimental levels are reproduced reasonably accurately, if we align the levels in such a way that the mean deviation in energy is zero. Because the levels in the energy region considered are still reasonably spaced, and most of the deviations are small, there is little doubt about the correctness of the assignments. The good agreement for the spectroscopic factors, as will be shown later, supports the identification. All levels, with the exception of the fourth 3^+ state, for which there is no unambiguous candidate, could be identified. The deviation in energy between experiment and theory in general is less than 200 keV. Only the 0^+ ground state, the 2_5^+ and the 3_3^+ state are off by more than this amount. It is remarkable that all other 0^+ states are reproduced very well, in contrast to the ground state.

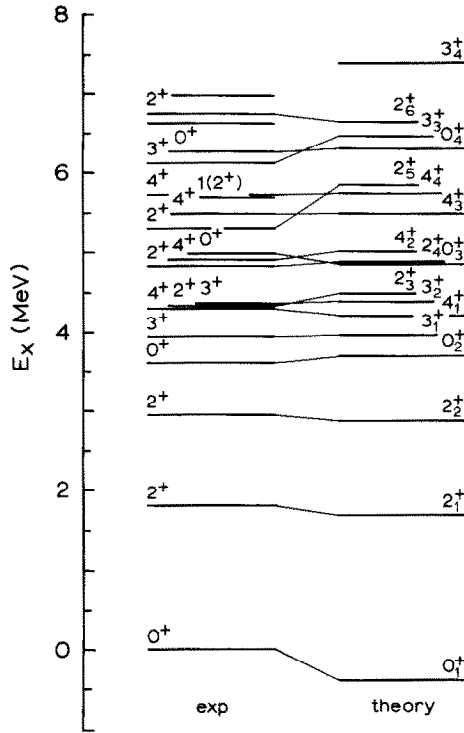


Fig. 5. A comparison between the first four experimental and theoretical positive-parity states of each spin in ^{26}Mg .

A more detailed test of the theoretical wave functions is given by a comparison of the spectroscopic factors. Therefore, spectroscopic factors for neutron transfer between the states considered and the ^{25}Mg ground state were determined. A problem is the fact that from the experimental angular distributions only the l -transfer can be deduced, so that the experiment cannot discriminate between a transfer to a $d_{3/2}$ or to a $d_{5/2}$ orbit in the case of a final state with $J^\pi = 2^+$ or 3^+ . The cross section for an $l = 2$ transfer, however, is the incoherent sum of a $d_{3/2}$ and a $d_{5/2}$ transfer and therefore can be written with the appropriate spin factors as

$$\left(\frac{d\sigma}{d\Omega}\right)_{\text{exp}}^{l=2} = 1.55 \frac{2J_f + 1}{2J_i + 1} \left[\frac{1}{4} S(d_{3/2}) \sigma^{\text{DWUCK}}(d_{3/2}) + \frac{1}{6} S(d_{5/2}) \sigma^{\text{DWUCK}}(d_{5/2}) \right].$$

Furthermore, within 1% independent from level energy in the energy region studied, $\sigma^{\text{DWUCK}}(d_{3/2}) = 1.78 \sigma^{\text{DWUCK}}(d_{5/2})$, which leads to the following expression for an $l = 2$ transfer:

$$\left(\frac{d\sigma}{d\Omega}\right)_{\text{exp}}^{l=2} = \frac{1.55}{4} \frac{2J_f + 1}{2J_i + 1} [S(d_{3/2}) + 1.19 S(d_{5/2})] \sigma^{\text{DWUCK}}(d_{3/2}).$$

The quantity $S(d_{3/2}) + 1.19S(d_{5/2})$ can easily be calculated both experimentally and theoretically. The results for the spectroscopic factors are summarized in table 3. As for the level scheme, the agreement is good, especially the relative importance of the different components of the wave functions is reproduced very nicely. It should be noted that the agreement between the absolute values of the

TABLE 3
Comparison between experimental and theoretical spectroscopic factors

$J^{\pi a)}$	E_x [MeV] ^{a)}	Assumed single-neutron state	$(2J+1)S^{\text{exp}}$	$(2J+1)S^{\text{theor}}$	
0_1^+	0	$d_{5/2}$	2.81		2.53
0_2^+	3.588	$d_{5/2}$	0.32		0.22
0_3^+	4.972	$d_{5/2}$	< 0.10		0.03
0_4^+	6.256	$d_{5/2}$	< 0.10		0.02
2_1^+	1.809	$s_{1/2}$	0.16		0.14
		$d_{3/2}$	3.51	0.05	
		$d_{5/2}$		1.61	1.97
2_2^+	2.938	$s_{1/2}$	3.37		1.93
		$d_{3/2}$	< 0.5	< 0.01	0.57
		$d_{5/2}$		0.48	
2_3^+	4.332 ^{b)}				
2_4^+	4.834	$s_{1/2}$	0.30		0.34
		$d_{3/2}$	1.05	0.12	
		$d_{5/2}$		0.36	0.54
2_5^+	5.291	$s_{1/2}$	< 0.01		< 0.01
		$d_{3/2}$	3.29	1.82	1.82
		$d_{5/2}$		< 0.01	
2_6^+	6.744	$s_{1/2}$	0.04		0.03
		$d_{3/2}$	0.58	< 0.01	
		$d_{5/2}$		0.42	0.50
3_1^+	3.941	$s_{1/2}$	1.98		1.70
		$d_{3/2}$	1.1	1.73	2.03
		$d_{5/2}$		0.25	
3_2^+	4.350 ^{b)}				
3_3^+	6.125	$s_{1/2}$	0.74		0.77
		$d_{3/2}$	4.2	2.07	2.35
		$d_{5/2}$		0.24	
4_1^+	4.318 ^{b)}				
4_2^+	4.900	$d_{3/2}$	1.48	1.02	1.04
		$d_{5/2}$		0.02	
4_3^+	5.474	$d_{3/2}$	2.15	0.87	1.91
		$d_{5/2}$		0.87	
4_4^+	5.716	$d_{3/2}$	0.56	0.05	0.73
		$d_{5/2}$		0.57	

The experimental spectroscopic factors are obtained for the neutron transfer indicated by the third column. The last column gives for $l = 2$ transfer the quantity $S(d_{3/2}) + 1.19S(d_{5/2})$ as discussed in the text.

^{a)} Ref. ⁹⁾. ^{b)} Unresolved triplet.

spectroscopic factors should be regarded with some caution since the DWBA calculations introduce an uncertainty in these values of around 20%. Nevertheless, detailed shell-model calculations seem able to describe at least the lowest four positive-parity states in quite some detail.

From the table it can be inferred that most of the strength to 0^+ states goes to the ground state, a result which is not surprising since the ground state will be an almost pure $\nu(d_{3/2})^6$ configuration coupled to the ¹⁶O core, completely filling the $d_{3/2}$ orbit. Higher 0^+ states will be relatively weak therefore, as is confirmed experimentally. Somewhat more surprising is the fact that most of the $s_{3/2}$ strength goes to the *second* 2^+ state (and the first 3^+ state), whereas the first 2^+ state predominantly is of a $d_{3/2}$ nature (according to the calculation), taking most of the remaining $d_{3/2}$ strength. From the table it can also be seen that in most mixed configurations (the 2^+ and 3^+ states), the largest component is systematically underestimated by a factor of 1.8. The unmixed transitions are much better reproduced. Apparently the shell model tends to mix the wave-function components slightly more than would seem necessary.

The sum rule for a neutron stripping reaction is given by

$$\sum_{\Gamma_{nlj}} \frac{2J_f + 1}{2J_i + 1} S(\Gamma_{nlj}) = \langle n^{-1} \rangle,$$

where the summation extends over all possible final states in a subshell (n, l, j) and $\langle n^{-1} \rangle$ is the number of neutron holes in the subshell. For the $s_{3/2}$ states, with $\sum (2J_f + 1)S(s_{3/2}) \leq 12$, we find experimentally for the left-hand expression: 6.59, somewhat more than half of the strength. Because of the ambiguity for $d_{3/2}$ and $d_{5/2}$ transfer in our experiment, we can for $l = 2$ transfer only deduce the total strength, which amounts to 21.25. Although the proton and neutron occupation numbers are not produced separately in the isospin formalism used in the calculations, the total occupation numbers ρ for the ground state of ²⁵Mg are given by $\langle \rho(s_{3/2}) \rangle = 0.88$, $\langle \rho(d_{3/2}) \rangle = 1.07$ and $\langle \rho(d_{5/2}) \rangle = 7.05$. Apparently the $s_{3/2}$ and $d_{3/2}$ orbits are hardly filled, whereas the $d_{5/2}$ orbit is about half full. Therefore the total $l = 2$ strength is observed in our experiment, but it seems that about 40% of the $s_{3/2}$ strength goes to higher excited states which were not observed in the experiment. From the fact that above 6.5 MeV excitation energy negative-parity states are observed increasingly, it would seem that most of the strength to the sd shell is exhausted and excitations to the $0f_{7/2}$ and $1p_{3/2}$ shells become important.

6. Conclusions

Accurate angular distributions were obtained with the ²⁵Mg(d, p)²⁶Mg reaction for most of the excited states in ²⁶Mg up to an excitation energy of 8 MeV. All

distributions could be satisfactorily described by standard DWBA calculations. Where J^π values were known, the deduced l -values are in agreement. Spin and parity restrictions could be obtained for the 7.262, 7.347, 7.543, 7.723, 7.771, 7.815 and 7.950 MeV levels. Extended shell-model calculations in the full sd shell reproduce both the excitation energies and the relative importance of the wave-function components rather well for the first four or six positive-parity states of each spin. The absolute magnitudes of the spectroscopic factors, however, of the mixed transfers were not calculated that well. In spite of the uncertainty in the magnitude of the spectroscopic factors deduced from the DWBA calculations, it may be concluded that in mixed configurations the largest component is systematically underestimated by the shell model. From the sum rule for $s_{\frac{1}{2}}$ transfers, finally, it would seem that only about 60% of the strength to this orbit is observed experimentally.

This work was performed as part of the research program of the "Stichting voor Fundamenteel Onderzoek der Materie" (FOM) with financial support from the "Nederlandse Organisatie voor Zuiver-Wetenschappelijk Onderzoek" (ZWO).

References

- 1) P. de Wit and P. M. Endt, private communication
- 2) D. Zwarts, G. A. Timmer and B. C. Metsch, Proc. Int. Conf. on nuclear structure, Amsterdam (1982), ed. A. van der Woude and B. J. Verhaar, vol. 1, p. 203
- 3) W. Chung, thesis, Michigan State University (1976), unpublished
- 4) H. W. Fulbright and J. R. Erskine, Nucl. Instr. Meth. **162** (1979) 355
- 5) C. P. M. van Engelen, R. O. Blaauboer and R. Kamermans, Nucl. Instr. Meth. **219** (1984) 529
- 6) P. D. Kunz, University of Colorado, internal report (unpublished)
- 7) C. M. Perey and F. G. Perey, At. Nucl. Data Tables **17** (1976) 2
- 8) F. D. Becchetti and G. W. Greenlees, Phys. Rev. **182** (1969) 1190
- 9) P. M. Endt and C. van der Leun, Nucl. Phys. **A310** (1978) 1
- 10) A. E. Champagne, A. T. Howard and P. D. Parker, Nucl. Phys. **A402** (1983) 159
- 11) W. P. Alford *et al.*, annual report McMaster Accelerator Laboratory (1983), p. 24
- 12) R. Hungerford and H. H. Schmidt, Nucl. Instr. Meth. **192** (1982) 609
- 13) E. Selin and R. Hardell, Nucl. Phys. **A139** (1969) 375